Advances in Social Science, Education and Humanities Research, volume 576
Proceedings of the 2nd International Conference on Science, Technology, and Modern Society (ICSTMS 2020)

The Crystal Structure and Magnetic Properties of Manganese Cobalt Ferrite ($Mn_{1-x}Co_xFe_2O_4$) Based on Natural Iron Sand and Used for Pb Ion Adsorption

N S Asri[1,*], E A Setiadi[1], Nurmadinah[2], M Addin[1], A P Tetuko[1], A Basyir[1], Rahmaniah[2], P Sebayang[1]
[1] Research Center for Physics, [2] Department of Physics
[1] Indonesian Institute of Sciences (LIPI), [2] Alauddin Islamic State University
[1] Banten, [2] Sulawesi Selatan, Indonesia
*nining.sumawati.asri@lipi.go.id, eko.arief.setiadi@lipi.go.id

***Abstract*—The manganese cobalt ferrite ($Mn_{1-x}Co_xFe_2O_4$) of x = 0.25, 0.50, and 0.75 have been synthesized to determine the structure and magnetic properties to be used as an adsorbent to remove Pb ions from aqueous solution. The material was prepared using the co-precipitation method and the removal process was performed by the adsorption method. The crystal structure, morphology and the magnetic properties were characterized using x-ray diffraction (XRD), surface electron microscopy (SEM), and vibrating sample magnetometer (VSM), respectively. The crystallite size of the material (by increasing the amount of Co content) was about 28.06, 27.97, and 26.61 nm, respectively. The morphology of the sample tends to agglomerate, with the grain protruding on its surface. Moreover, the VSM analysis shows that the saturation magnetizations improve as the x value increased, while its coercivity was decreased which showed a superparamagnetic behavior. Further, the adsorption of Pb ions was analyzed using an atomic absorption spectroscopy (AAS). The result showed that the maximum adsorption capacity was obtained around 290.5 mg/g with an efficiency of 82.30 %. Therefore, this material has the potential application to be used as an adsorbent to remove the metal ions from wastewater.**

Keywords*—crystal structure, magnetic properties, manganese cobalt ferrite

I. INTRODUCTION

Ferrite is an interesting material due to its unique properties, such as high thermal permeability and resistivity as well as its small coercivity [1]. Ferrite is known as a soft-magnetic material that has a spinel structure. The chemical formula of ferrite is $M\text{-}Fe_2O_4$, where M is a divalent metal ion, such as Cu, Zn, Ni, Co, Fe, Mn, and Mg. Besides, ferrite materials have strong mechanical properties, high stability on the external field, and temperature [2]. Ferrites are widely promising in many applications, such as in medical sector to be used as immobilization and breakdown medium of the enzyme and protein, and drug delivery system. On the other hand, ferrite can be applied as a heavy metal adsorbent for wastewater [3], ferrofluid [4], and sensor technology [5]. The possibility of changing the divalent cations (M^{2+}) in the ferrite crystallography is the way to arrange the magnetic and the electrical properties [6].

Ferrite materials have been synthesis with various methods, such as sol-gel [7], hydrothermal [8], solid-state spin coating [9], and co-precipitation [3]. Among all of those methods, chemical co-precipitation is the most efficient due to its simplicity and can be produced in relatively low temperatures [1]. Moreover, co-precipitation method is one of the best methods to control the crystal structures and magnetic properties of materials [10]. To be used in a heavy metal adsorption application, the optimum condition could be achieved by reducing the grain size of the adsorbent, thus the surface area is enhanced, and the active sites are increased. Further, the small coercivity and high saturation magnetization also contribute to adsorption efficiency [11].

The spinel manganese ferrite ($MnFe_2O_4$) is generally a soft magnetic which relatively has a high surface area with good chemical stability [12], high saturation magnetization and low coercivity [13]. Mn^{2+} ion on the tetrahedral sites can be doped with d-block transition elements, such as Co, Ni, Zn, and Cu to improve the magnetic properties and to control the particle size of $MnFe_2O_4$ as a superparamagnetic material [14]. The composite material synthesis that contains two or more metal ferrite is challenging, particularly to find its new materials characteristic which can be applied for widely applications.

In this study, we focus on the synthesis of $Mn_{1-x}Co_xFe_2O_4$ ferrite materials from natural iron sand with variations of x = 0.25, 0.50, and 0.75 using a co-precipitation method by modifying the divalent ion which combines Co^{2+} and Mn^{2+}. Iron sand is known as an abundant natural material in Indonesia that contains a high iron element. Further, the material was used as an adsorbent to remove Pb ions from an aqueous solution. The analysis of material properties was performed using x-ray diffraction (XRD), surface electron spectroscopy (SEM), and vibration sample magnetometer (VSM). The adsorption capacity of heavy metal ions (Pb) is analyzed using atomic absorption spectroscopy (AAS).

II. METHODS

The $Mn_{1-x}Co_xFe_2O_4$ were synthesized from natural sand which provides Fe^{3+} ions, taken from the Jeneberang River (Gowa, South Sulawesi). $MnCl_2$ and $CoCl_2$ (purchased from Merck) as the chemical precursor provide Mn^{2+}/Co^{2+} ions. The synthesis process was conducted using a co-precipitation method with three variations of x = 0.25, 0.5, and 0.75. The first step was performed by dissolving 8 gr of the iron sand into 50 mL of HCl solution (37%), then the solution was filtered to obtain the cationic solution of Fe^{3+}. Further, $MnCl_2$ and $CoCl_2$ were added into the filtered solution with mole ratio of 0.75:0.25; 0.5:0.5 and 0.25:0.75, respectively, and stirred to obtain a homogenous solution. Then, the mixture solution was dropped slowly into 4 M NH_4OH, followed by stirring the mixture solution using a speed of 250 rpm for 2 hours at 70°C. Furthermore, after the precipitation was formed, the solution was separated from the precipitate and washed several times using aquadest to remove any impurities. The samples which have been successfully synthesized were dried at 80°C. On the other hand, the Pb ions adsorption process was carried out by mixing 2 mg/mL of $Mn_{1-x}Co_xFe_2O_4$ powder into wastewater which contains the Pb ions. Then the mixture was shaked using a shaker mill for 30 minutes.

The crystalline phase of $Mn_{1-x}Co_xFe_2O_4$ was characterized by x-ray diffractometer (XRD – Rigaku Smartlab) with Cu Kα (λ = 1.5418 Å). The morphology of the sample was analyzed by surface electron microscopy (SEM-Hitachi). The magnetic properties of the samples were obtained from a vibrating sample magnetometer (VSM; Dexing 250), and the concentration of Pb ions before and after the adsorption were measured using ASS (AAS – Shimadzu AA6800).

III. RESULTS AND DISCUSSION

The XRD patterns of $Mn_1\text{-}xCo_xFe_2O_4$ (x = 0.25, 0.50 and 0.75) are shown in Figure 1. The hkl indices and the characteristic peaks of the samples corresponds to (220), (311), (222), (511) and (440) planes that indicate the cubic spinel ferrite structure as per PDF card no. 74-2403 ($MnFe_2O_4$) [15] and 22-1086 ($CoFe_2O_4$) [16]. However, the other peaks arise by increasing the addition of Co^{2+} substitution which was identified as a hematite phase (Fe_2O_3). The presence of impurity on the mixed ferrite might due to an incomplete crystallization step in the atomic level of the sample. The metal cation which was attracted to OH^- forms a hydroxide compound. However, if the hydroxide fails to form ferrite nanoparticles a further oxidation state (Fe_2O_3) could occurs [17].

Based on the XRD result, several variables can be analyzed, such as the lattice parameter (*a*), the crystallite size (D), dislocation density (δ) and lattice strain (ε) which are shown in Table 1. Those variables were calculated from the main peak of the samples (311), as presented in equations 1 – 4 [1,18,19].

$$a^2 = \frac{\lambda^2}{4\sin^2\theta}(h^2 + k^2 + l^2) \quad (1)$$

$$D = \frac{\kappa\lambda}{\beta\cos\theta} \quad (2)$$

$$\delta = \frac{1}{D^2} \quad (3)$$

Where *a* is the lattice parameter, D is the crystallite size, κ is the Scherrer constant (0.89), λ is the wavelength of the X-ray, β is the full width at half maximum (FWHM) from the main peak, δ is the dislocation density and ε is the lattice strain.

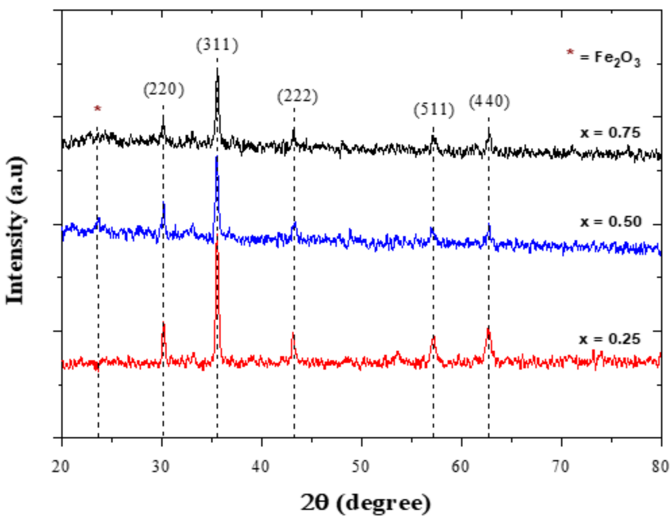

Fig. 1. XRD pattern of $Mn_{1-x}Co_xFe_2O_4$.

TABLE I. XRD ANALYSIS: LATTICE PARAMETER (A), CRYSTALLITE SIZE (D), DISLOCATION DENSITY (δ) AND LATTICE STRAIN (ε) OF $MN_{1-x}CO_xFE_2O_4$ WITH X = 0.25, 0.50 AND 0.75

Samples	*a* (Å)	D (nm)	δ ($x10^{15}$line/m^2)	ε ($x10^{-3}$)
x = 0.25	8.398	28.06	1.27	4.01
x = 0.50	8.393	27.97	1.28	4.03
x = 0.75	8.390	26.62	1.41	4.23

The lattice parameter (Table 1) decreases as the Co content increased where the lattice parameter also affects the crystallite size reduction. The decrease in lattice parameters could be attributed to the different ionic radii of Mn^{2+} and Co^{2+}. The ionic radii of Mn^{2+} (r = 0.83 Å) [20] was replaced by the smaller ionic radii of Co^{2+} (r = 0.745 Å) [19], thus the crystallite structure was decreased due to the constriction of the unit cell. A similar case was also reported by Mubarokah *et al* [19], Yadav *et al* [21] and Sharifi *et al* [22]. The addition of Co^{2+} also influences the dislocation density and lattice strain of $Mn_{1-x}Co_xFe_2O_4$ crystallography system. According to Figure 1, the increasing of Co^{2+} content affected the presence of a secondary phase (impurity peak) which is recognized as hematite. Eventually, it brings on an enhancement of the dislocation density and the lattice strain numbers because of the deformation and the failure at the crystallography system in $Mn_{1-x}Co_xFe_2O_4$ [19,23].

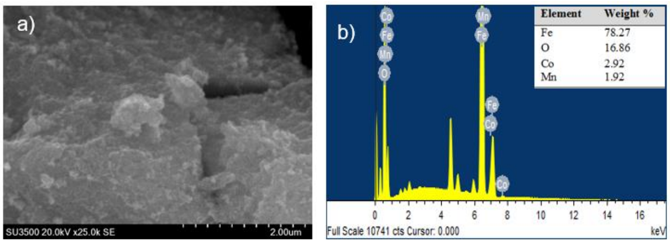

Fig. 2. (a) SEM image and (b) EDS analysis of $Mn_{1-x}Co_xFe_2O_4$ (x = 0.75).

The morphology of $Mn_{1-x}Co_xFe_2O_4$ sample was characterized using SEM-EDS, particularly the sample with x = 0.75, and the image is shown in Figure 2 (a). The sample tends to agglomerate with an unclear shape of a sphere on the surface. The EDS (energy dispersive spectroscopy) of the sample is presented in Figure 2 (b). The composition was obtained from the analysis: Fe (78.27 wt.%), O (16.86 wt.%), Co (2.92 wt.%) and Mn (1.92 wt.%). Based on the analysis, the EDS confirmed that Co^{2+} content has a higher value compared to Mn^{2+} according to the composition ratio of Co^{2+} and Mn^{2+} (0.75: 0.25).

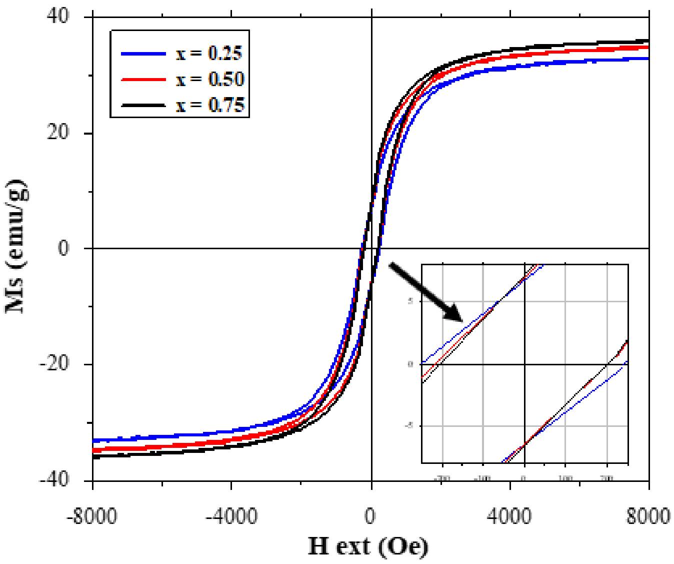

Fig. 3. The hysteresis loops of $Mn_{1-x}Co_xFe_2O_4$.

The magnetic properties of materials were measured using a vibrating sample magnetometer (VSM) and the hysteresis curves are shown in Figure 3. The increasing of Co^{2+} content that was substituted on the Mn^{2+} sites has an effect on the saturation magnetization (*Ms*) improvement and the coercivity (*Hc*) reduction. The narrow and linear shape on the hysteresis curves showed the superparamagnetic dominant when the Co^{2+} content increased [24]. Moreover, the superparamagnetic behavior achieved when the material was obtained as a nano-crystallite size sample. The large surface area in a nanosize material affects the anisotropic energy reduction and generates a single domain. The consequence is the magnetic moment inside the particles could rotate simultaneously following the direction of the external magnetic field which resulted to the smaller coercivity value [25]. The overall values of the magnetic properties and its relation with crystallite size of $Mn_{1-x}Co_xFe_2O_4$ are summarized in Table 2.

TABLE II. RELATION OF CRYSTALLITE SIZE D, COERCIVITY *HC*, SATURATION MAGNETIZATION *MS*, AND REMANENT MAGNETIZATION *MR* OF $MN_{1-x}CO_xFE_2O_4$ SAMPLES

Sample	D (nm)	*Hc* (Oe)	*Ms* (emu/g)	*Mr* (emu/g)
x = 0.25	28.06	247.24	33.90	6.61
x = 0.50	27.97	218.41	35.83	6.98
x = 0.75	26.62	208.24	36.70	7.31

To investigate the adsorption capacity (q_e) and removal efficiency (*R*) of Pb ion using $Mn_{1-x}Co_xFe_2O_4$ with different value of Co^{2+} substitution, we analyzed the aqueous solution using atomic absorption spectroscopy (AAS) and we calculated the parameters using the following equations [16]:

$$q_e = \frac{(C_i - C_e)}{m} V \tag{5}$$

$$R(\%) = \frac{C_i - C_e}{C_e} \times 100 \tag{6}$$

Where C_i and C_e (mg/l) are initial and equilibrium concentrations of Pb ions, V (l) is the volume of the solution, and m (g) is the mass of nanoparticles adsorbent.

The results of AAS analysis are presented in Table 3. The adsorption capacity was increased as the Co^{2+} ion substitution escalated the addition of Co^{2+} affects the crystallite size reduction of the sample. Larger surface area could be obtained on smaller particles. This means, the active site on the surface also improved to adsorb the metal ion in the wastewater [26].

TABLE III. PB ION ADSORPTION USING $MN_{1-x}CO_xFE_2O_4$ WITH X = 0.25, 0.50 AND 0.75

x	D (nm)	C_i (mg/L)	C_e (mg/L)	q_e (mg/g)	R (%)
0.25	28.06	706	281	212.5	60.20
0.50	27.97	706	153	276.5	78.33
0.75	26.62	706	125	290.5	82.30

IV. CONCLUSION

$Mn_{1-x}Co_xFe_2O_4$ (x = 0.25, 0.50, 0.75) samples synthesized from natural iron sand as the raw material have been successfully produced using a co-precipitation method. The crystal structure showed a cubic spinel structure with a slightly presence of a secondary phase (Fe_2O_3) along with the addition of x value. The calculated crystallite size of all samples is within a range of 26.62 – 28.06 nm, where the size of crystal decreased as the Co^{2+} content increased. The sample with x = 0.75 showed a morphology which tend to be agglomerated on its surface. Further, the VSM analysis showed the quite narrow hysteresis for all samples. The saturation magnetization exhibits an enhancement by the addition of Co^{2+} while the coercivity was decreased. The $Mn_{1-x}Co_xFe_2O_4$ samples could be used as an adsorbent for Pb ions, and the maximum adsorbent capacity obtained is about 290.5 mg/g with the efficiency 82.30% at the sample of x = 0.75.

ACKNOWLEDGMENTS

This publication was supported by National Innovation System Research Program (INSINAS) 2020 of the Ministry of Research and Technology of the Republic of Indonesia (RISTEK-BRIN).

REFERENCES

[1] E.A. Setiadi, S. Simbolon, M. Yunus, C. Kurniawan, A.P. Tetuko, S. Zelviani, and P. Sebayang, "The Effect of Synthesis Temperature on Physical and Magnetic Properties of Manganese Ferrite (MnFe2O4) Based on Natural Iron Sand," in Journal of Physics: Conference Series, 2018, vol. 979, no. 1, p. 12064.

[2] A. Khuriati, Y. Astanto, and H. Traningsih, "Efek Aditiv Al2O3 Terhadap Struktur Dan Sifat Fisis Magnet Permanen BaO. 6 (Fe2O3)," Berk. Fis., vol. 7, no. 2, pp. 69–73, 2004.

[3] N.S. Asri, F.A. Nurdila, T. Kato, S. Iwata, and E. Suharyadi, "Removal Study of Cu (II), Fe (II) and Ni (II) Ions from Wastewater Using Polymer-Coated Cobalt Ferrite (CoFe2O4) Magnetic Nanoparticles Adsorbent," in Journal of Physics: Conference Series, 2018, vol. 1091, no. 1, p. 12016.

[4] D. Ramimoghadam, S. Bagheri, and S.B. Abd Hamid, "Stable Monodisperse Nanomagnetic Colloidal Suspensions: An Overview," Colloids Surfaces B Biointerfaces, vol. 133, pp. 388–411, 2015.

[5] A. Šutka and K.A. Gross, "Spinel Ferrite Oxide Semiconductor Gas Sensors," Sensors Actuators B Chem., vol. 222, pp. 95–105, 2016.

[6] G. Datt and A.C. Abhyankar, "Dopant Driven Tunability of Dielectric Relaxation in MxCo (1-x) Fe2O4 (M: Zn2+, Mn2+, Ni2+) Nano-Ferrites," J. Appl. Phys., vol. 122, no. 3, p. 34102, 2017.

[7] A. Hussain, T. Abbas, and S.B. Niazi, "Preparation of Ni1−XMnxFe2O4 Ferrites by Sol–Gel Method and Study of Their Cation Distribution," Ceram. Int., vol. 39, no. 2, pp. 1221–1225, 2013.

[8] K. Nejati and R. Zabihi, "Preparation and Magnetic Properties of Nano Size Nickel Ferrite Particles Using Hydrothermal Method," Chem. Cent. J., vol. 6, no. 1, pp. 1–6, 2012.

[9] Y. Yusuf and M.S. Mustaffa, "Spin-Coating Technique for Fabricating Nickel Zinc Nanoferrite (Ni0. 3Zn0. 7Fe2O4) Thin Films," in Coatings and Thin-Film Technologies, IntechOpen, 2018.

[10] Y.B. Kannan, R. Saravanan, N. Srinivasan, K. Praveena, and K. Sadhana, "Synthesis and Characterization of Some Ferrite Nanoparticles Prepared by Co-Precipitation Method," J. Mater. Sci. Mater. Electron., vol. 27, no. 11, pp. 12000–12008, 2016.

[11] E.A. Setiadi, P. Sebayang, M. Ginting, A.Y. Sari, C. Kurniawan, C.S. Saragih, and P. Simamora, "The Synthesization of Fe3O4 Magnetic Nanoparticles Based on Natural Iron Sand by Co-Precipitation Method for the Used of the Adsorption of Cu and Pb Ions," in Journal of Physics: Conference Series, 2016, vol. 776, no. 1, p. 12020.

[12] L.A. Kafshgari, M. Ghorbani, and A. Azizi, "Synthesis and Characterization of Manganese Ferrite Nanostructure by Co-Precipitation, Sol-Gel, and Hydrothermal Methods," Part. Sci. Technol., 2018.

[13] J.A. M., U. V, N. P, and R.S. R, "Synthesis and Comparative Studies on MnFe2O4 Nanoparticles with Different Natural Polymers by Sol-Gel Method : Structural, Morphological, Optical, Magnetic, Catalytic, and Biological Activities," J. Nanostructure Chem., pp. 1–13, 2017.

[14] E.R. Kumar, P.S.P. Reddy, G.S. Devi, and S. Sathiyaraj, "Structural, Dielectric and Gas Sensing Behavior of Mn Substituted Spinel MFe2O4 (M= Zn, Cu, Ni, and Co) Ferrite Nanoparticles," J. Magn. Magn. Mater., vol. 398, pp. 281–288, 2016.

[15] K. Zipare, J. Dhumal, S. Bandgar, V. Mathe, and G. Shahane, "Superparamagnetic Manganese Ferrite Nanoparticles: Synthesis and Magnetic Properties," J. Nanosci. Nanoeng., vol. 1, no. 3, pp. 178–182, 2015.

[16] N.S. Asri and E. Suharyadi, "Preparation of CoFe2O4/SiO2 Magnetic Nanoparticles as Adsorbent of Ni and Cu Ions from Aqueous Solution," in AIP Conference Proceedings, 2020, vol. 2256, no. 1, p. 30022.

[17] N. Siregar, I.P.T. Indrayana, E. Suharyadi, T. Kato, and S. Iwata, "Effect of Synthesis Temperature and NaOH Concentration on Microstructural and Magnetic Properties of Mn0. 5Zn0. 5Fe2O4 Nanoparticles," in IOP Conference Series: Materials Science and Engineering, 2017, vol. 202, no. 1, p. 12048.

[18] R. Mimouni, K. Boubaker, and M. Amlouk, "Investigation of Structural and Optical Properties in Cobalt–Chromium Co-Doped ZnO Thin Films within the Lattice Compatibility Theory Scope," J. Alloys Compd., vol. 624, pp. 189–194, 2015.

[19] Z.R. Mubarokah, P. Sebayang, A.P. Tetuko, and E.A. Setiadi, "Synthesis of Mn1-XNixFe2O4 Magnetic Materials Using Natural Iron Sand Prepared by Co-Precipitation Method," in AIP Conference Proceedings, 2020, vol. 2296, no. 1, p. 20135.

[20] R.D. Shannon, "Revised Effective Ionic Radii and Systematic Studies of Interatomic Distances in Halides and Chalcogenides," Acta Crystallogr. Sect. A Cryst. physics, diffraction, Theor. Gen. Crystallogr., vol. 32, no. 5, pp. 751–767, 1976.

[21] A. Yadav and D. Varshney, "Structural and Temperature Dependent Dielectric Behavior of Cr and Zn Doped MnFe2O4 Nano Ferrites," Superlattices Microstruct., vol. 113, pp. 153–159, 2018.

[22] S. Sharifi, A. Yazdani, and K. Rahimi, "Incremental Substitution of Ni with Mn in NiFe 2 O 4 to Largely Enhance Its Supercapacitance Properties," Sci. Rep., vol. 10, no. 1, pp. 1–15, 2020.

[23] S.N. Adarakatti, V.S. Pattar, P.K. Korishettar, B. V Grampurohit, R.G. Kharabe, A.B. Kulkarni, S.N. Mathad, C.S. Hiremath, and R.B. Pujar, "Synthesis, Structural and Electrical Studies of Li-Ni-Cu Nano Ferrites," Acta Chem. Iasi, vol. 26, no. 1, pp. 1–12, 2018.

[24] L.A. Kafshgari, M. Ghorbani, and A. Azizi, "Fabrication and Investigation of MnFe2O4/MWCNTs Nanocomposite by Hydrothermal Technique and Adsorption of Cationic and Anionic Dyes," Appl. Surf. Sci., vol. 419, pp. 70–83, 2017.

[25] M.G. Naseri and E.B. Saion, "Crystalization in Spinel Ferrite Nanoparticles," Adv. Cryst. Process., pp. 349–380, 2012.

[26] L. Ai, Y. Zhou, and J. Jiang, "Removal of Methylene Blue from Aqueous Solution by Montmorillonite/CoFe2O4 Composite with Magnetic Separation Performance," Desalination, vol. 266, no. 1–3, pp. 72–77, 2011.